

Laser ablation of nanoscale particles with 193 nm light

This article has been downloaded from IOPscience. Please scroll down to see the full text article.

2007 J. Phys.: Conf. Ser. 59 54

(<http://iopscience.iop.org/1742-6596/59/1/012>)

[The Table of Contents](#) and [more related content](#) is available

Download details:

IP Address: 128.32.10.179

The article was downloaded on 06/04/2010 at 21:36

Please note that [terms and conditions apply](#).

Laser ablation of nanoscale particles with 193 nm light

J H Choi¹, D Lucas², and C P Koshland³

¹Mechanical Engineering, University of California, Berkeley, CA 94720, USA

²Lawrence Berkeley National Laboratory, CA 94720, USA

³School of Public Health, University of California, Berkeley, CA 94720, USA

Email: jhyunc@me.berkeley.edu, d_lucas@lbl.gov

Abstract. Laser interaction with nanoscale particles is distinct and different from laser-bulk material interaction, where a hot plasma is normally created. Here, we review our studies on 193 nm laser ablation of various nanoscale particles including NaCl, soot, polystyrene, and gold. The 20 ns laser beam with fluences up to 0.3 J/cm² irradiates nanoparticles in a gas stream at laser repetition rates from 10 to 100 Hz. The particle size distributions before and after irradiation are measured with a scanning mobility particle sizer (SMPS), and particle morphology is examined with electron microscopy. All the nanomaterials studied exhibit a similar disintegration pattern and similar particle formation characteristics. No broadband emission associated with particle heating or optical breakdown is observed. The nanoparticles formed after irradiation have a smaller mean diameter and an order of magnitude higher number concentration with a more spherical shape compared to the original particles. We use the photon-atom ratio (PAR) to interpret the laser-particle interaction energetics.

1. Introduction

Laser ablation is often used for chemical analysis and material processing of solid surfaces, where materials are normally removed in a hot plasma created by intense laser radiation. Laser ablation is also used to synthesize nanoparticles, but nano- to microscale fractal agglomerates are often generated. The underlying physical processes are not well understood, and a wide size spectrum of particles as well as gas phase species are produced in the high temperature plasma [1,2]. In addition, various parameters, including laser wavelength and intensity, pulse duration, and the optical properties of target materials affect the nature of the laser-material interactions and plasma generation.

The laser interaction with nanoscale materials is distinct and different from laser-bulk material systems; one example is that the optical breakdown threshold of nanoparticles is higher than that of bulk solids by a factor of 10 to 100 [3]. In our previous studies, plasmas were formed at $\sim 10^9$ W/cm² by 193 nm laser irradiation of 110 nm polystyrene spheres, whereas bulk Pb(NO₃)₂ and polystyrene surfaces had thresholds one to two orders of magnitude lower, respectively [4,5]. The nanoparticles and bulk solids, however, exhibited similar optical characteristics below the breakdown thresholds; atomic fluorescence was detected with a decay time of ~ 10 ns and no long lifetime broadband incandescence associated with laser heating was observed. When we used 532 nm light instead of 193 nm light at similar fluences, incandescence was observed from the same particles, confirming that thermal effects are negligible in the 193 nm laser ablation of nanoparticles. We observed fluorescence of carbon atoms from 193 nm irradiation of polystyrene and soot particles [5]. Both fluorescence signals exhibited linear, intermediate, and saturation regimes with increasing fluence, but the signal

from polystyrene increased faster and saturated at lower fluences, indicating that the extent of disintegration of the different particles varies because of different particle material and size. When plotted against a dimensionless ratio, called the photon-to-atom ratio (PAR), the signals from both particles fall into a single curve.

Here, we review our recent studies [6-9] on 193 nm laser ablation of nanoscale polystyrene, soot, NaCl, and gold particles in a constrained gas stream. These particles are chosen because they represent different classes of materials, and their size distributions and morphology are different. The 20 ns pulses at 193 nm ablate the particles into gas phase species at fluences two orders of magnitude below the breakdown threshold; the species subsequently condense to form a new mode of nanoparticles whose size and morphology can be controlled. The purpose of this paper is to extract a general scheme in UV laser ablation/processing of different nanomaterials and suggest analysis tools. We assess the differences and similarities in ablation and production processes of these nanoparticles using the PAR.

2. Experiments

The experimental apparatus for the laser ablation of nanoparticles was described previously [6-9]. Soot particles are generated from a CH₄-air nonpremixed flame, while polystyrene, gold, and NaCl particles are produced from a nebulizer (BGI, CN-24). Particles in air or N₂ enter the laser interrogation region at either 0.3 or 2.0 standard liters per minute (slpm). The 20 ns long 193 nm pulses from an ArF excimer laser (Lambda Physik, 210i) are delivered by a 3.8 cm diameter, 25 cm focal length CVI lens. The 1 cm wide and 0.5 cm high beam irradiates a 1×1×4 cm³ quartz cuvette that constrains the particle-laden flow. Laser fluences up to 0.3 J/cm² are used with repetition rates from 10 to 100 Hz. At different laser repetition rates and flow rates, each particle is hit by a single pulse or multiple shots while flowing through the cuvette. The size distributions of the irradiated particles are measured by a scanning mobility particle sizer (SMPS, TSI 3071A/3025A), which assumes spherical particles being probed. The overall uncertainty in size distribution measurements is within 15%. Particles are also collected downstream of the cuvette for morphology analysis with electron microscopy.

3. Results

The size distributions of polystyrene, soot, and NaCl nanoparticles irradiated by 193 nm light at the laser fluences of 0, 0.07, and 0.14 J/cm² are shown in Fig. 1. While flowing through the cuvette, the particles are hit on average by a single laser shot. The particle number densities of the three polystyrene distributions are increased by a factor of 5 for comparison. The experimental conditions and relevant data are summarized in Table 1. The nearly monodisperse polystyrene spheres have an original diameter of 110 nm, whereas the soot, NaCl, and gold particles are polydisperse agglomerates with mean diameters of 265, 118, and 39 nm, respectively. The number concentrations of polystyrene, soot, NaCl, and gold particles are approximately 5×10⁴, 5×10⁵, 2×10⁶, 2×10⁵ cm⁻³, respectively. Laser ablation significantly modifies the size distributions of all these particles, generating smaller particles at higher concentrations than the original particles. For all types of particles studied, the mean diameter and number concentration increase as the laser fluence increases. The volume of the irradiated soot and polystyrene particles decreases by 10 to 31% from the original volume, whereas the volume of NaCl and gold is conserved within the experimental error.

When the particles are ablated by multiple laser shots at the same range of laser fluences (Table 1), a drastic change is observed. The mean diameter of polystyrene and soot particles decreases from 27 to 20 nm and from 51 to 31 nm with increasing fluence, with a corresponding decrease in number concentrations. The particle volume of polystyrene and soot decreases by 85 and 90% from the original particle volume. The volume loss of soot is caused by oxidation, whereas polystyrene volume is lost because of the formation of particles smaller than 13 nm (the smallest particle diameter measured at this operating condition) and/or stable gas phase species that do not condense. In contrast, the particle diameter of NaCl continues increasing from 27 to 43 nm with an increasing number concentration, since NaCl does not oxidize and the vapor pressure of NaCl is extremely small.

Figure 2 shows the morphology of the soot and gold particles irradiated at 0.18 J/cm^2 . The original soot has an agglomerated shape with a fractal dimension (D_f) near 1.8, composed of $\sim 40 \text{ nm}$ spherical primary particles. After irradiation, spherical agglomerates ($D_f \sim 3$) dominate and most of the particles consist of $\sim 40 \text{ nm}$ spheres. The original NaCl particles have a structure similar to soot [7]. Fractal agglomerated NaCl particles also become spherical clusters composed of $\sim 40 \text{ nm}$ spheres after irradiation. In contrast, the irradiated gold nanoparticles are individual spheres with a diameter of $\sim 7 \text{ nm}$ (Fig. 2(b)). Spheres with a mean diameter of $\sim 23 \text{ nm}$ are also observed with polystyrene after irradiation at 0.12 J/cm^2 [8]. The electron microscope images of all particles examined are qualitatively consistent with the SMPS results.

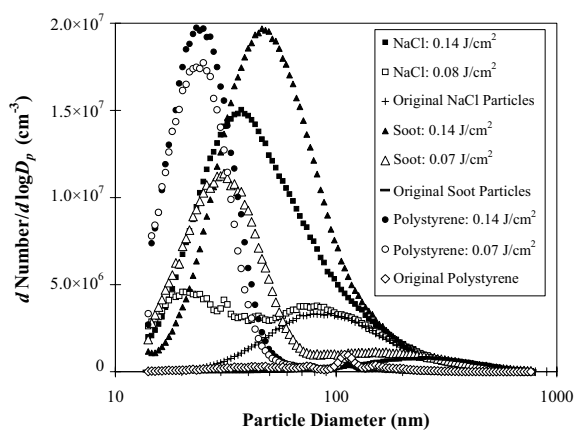


Figure 1. Size distributions of polystyrene, soot, and NaCl particles irradiated by a single 193 nm laser shot. Note that the number densities in three polystyrene distributions are increased by a factor of 5 for comparison.

Particles	Fluence (J/cm^2)	# of shot /particle	PAR	Diameter (nm)	Number (cm^{-3})	Volume (nm^3/cm^3)
Polystyrene	-	-	-	110	5.2×10^4	6.9×10^{10}
in N_2	0.07	1	0.03	22	1.2×10^6	5.4×10^{10}
	0.14	1	0.07	25	1.4×10^6	4.7×10^{10}
	0.07	5	0.17	27	1.8×10^6	2.8×10^{10}
	0.14	5	0.33	20	7.6×10^5	9.6×10^9
Soot	-	-	-	265	4.5×10^5	8.6×10^{12}
in air	0.07	1	0.03	31	5.6×10^6	7.7×10^{12}
	0.14	1	0.08	48	1.1×10^7	7.7×10^{12}
	0.07	8	0.16	51	8.6×10^6	5.1×10^{12}
	0.14	8	0.40	31	4.8×10^6	8.0×10^{11}
NaCl	-	-	-	118	2.2×10^6	7.1×10^{12}
in air	0.08	1	0.08	20	4.1×10^6	6.9×10^{12}
	0.14	1	0.15	37	9.4×10^6	7.6×10^{12}
	0.08	8	*	27	7.9×10^6	7.5×10^{12}
	0.14	8	*	43	1.5×10^7	7.5×10^{12}
Gold	-	-	-	39	2.2×10^5	1.9×10^{10}
in air	0.07	1	0.18	< 5	6.1×10^5	1.9×10^{10}
	0.12	1	0.34	6	1.1×10^6	1.6×10^{10}

Table 1. Experimental conditions and data for 193 nm laser ablation of various nanomaterials. Note that gold particles are measured in a size window of 5–200 nm, while other particles are monitored in the range from 13 to 800 nm. (*see text)

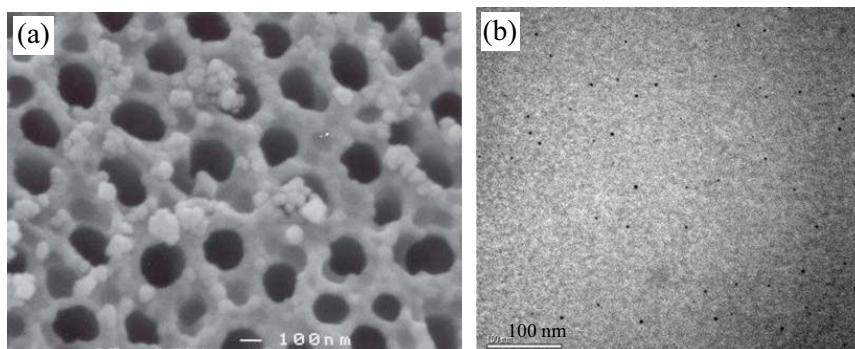


Figure 2. Electron micrographs of soot (a) and gold (b) particles irradiated by 193 nm light at 0.18 J/cm^2 , corresponding to a PAR = 0.48 for soot (8 shots/particle) and a PAR = 0.49 for gold (1 shot/particle). Note that the filter pore size in (a) is $\sim 200 \text{ nm}$.

4. Discussion

The 193 nm laser ablation decomposes the nanoparticles primarily through a photochemical process rather than thermal desorption, as it produces no broadband emission associated with particle heating or optical breakdown. The temperature increase of nanoparticles during 193 nm laser irradiation is on the order of 100 K [9]. This is consistent with Garrison and Srinivasan [10] who observed no surface melting when 193 nm light photolytically ablated bulk surfaces at similar fluences. All the nanomaterials studied in our lab exhibit a similar fragmentation pattern; a portion of each particle is disintegrated into gas phase species by absorption of the UV photons, and fluorescence of gas phase species is produced from the particles [5,7,11]. To evaluate the extent of disintegration of different particles, we use the photon-to-atom ratio (PAR), a ratio of the number of absorbed photons to the number of atoms in the particle. PAR is a more relevant metric than laser fluence to understand laser-particle interactions, because PAR accounts for the energy balance of each particle whereas the fluence is more suited for homogeneous media such as gases or bulk solids. We carry out Mie scattering calculations [12] to determine the fraction of incident photons that are absorbed by the particles. A 110 nm polystyrene particle absorbs approximately 57% of photons striking the particle, while about 80 and 88% are absorbed by 265 nm soot and 39 nm gold particles, respectively. NaCl absorbs 193 nm light by a two-photon process, but the two-photon absorption cross-section of NaCl at 193 nm is unknown, so we assume that all the photons striking the particles are absorbed for the calculation. The PAR values for the experimental conditions are presented in Table 1 and Fig. 2. For multiple shot irradiation, the PARs presented are simply multiplied by the number of laser shots per particle, since adding energy to a particle with multiple pulses likely disintegrates the particle to a different extent than depositing the same amount of energy in one pulse, and the specific status of the particles after each individual pulse is unknown.

Our previous measurements of atomic carbon fluorescence from the 193 nm laser ablation of polystyrene and soot nanoparticles suggested that particles with different materials and sizes are fully disintegrated at a $\text{PAR} \geq 3$ [5]. The theoretical threshold for full disintegration is a $\text{PAR} = 1$ since each laser photon has a greater energy than average bond energy in the particles. If we consider liberation of carbon atoms and electronic excitation (resonant with 193 nm light), the PAR threshold for complete disintegration is between 1 and 3. Most of the polystyrene and soot particle volume is lost as the PAR approaches unity (Table 1). The photolyzed species that are not lost condense to form new smaller particles at an order of magnitude higher concentration. When we irradiated NaCl particles with an initial mean diameter of 26 nm at similar fluences, the size distributions of the irradiated particles were almost identical to the original distribution [7]. Here, the original particles were fully disintegrated into gas phase species since the PARs were all above unity, and self-preserving size distributions were formed since the species experienced the similar condensation condition to where the particles initially formed.

When polystyrene size distributions at different laser conditions were non-dimensionalized using number and volume concentrations, a universal size distribution was observed, suggesting that the irradiated particles are formed by the same mechanism [8]. The nanospheres observed with the irradiated polystyrene and gold indicate that these particles are formed by nucleation of the photolyzed species rather than fracture of the original particles. Since all the PARs used in these cases are less than unity, the original particles cannot be completely disintegrated, and the photolyzed species can also condense on the remaining particle fragments. Therefore, particles are formed by both homogeneous and heterogeneous nucleation, but we could not differentiate these processes since the channel resolution of the SMPS is not sufficiently high. For instance, ablation of a single 110 nm polystyrene sphere at a $\text{PAR} = 0.03$ produces gaseous species and the original sphere becomes approximately 108 nm in diameter, assuming a perfect photochemistry with a yield of unity. The channel resolution at this particle diameter is approximately 5%, so the remaining particle cannot be identified from the original particle.

The nucleated nanospheres are likely to have the same charge as a result of UV photoelectron production, rather than a bipolar Boltzmann charge distribution. Thus, agglomeration is suppressed,

which was also observed with the nanoparticles produced from laser ablation of micron-size particles with 248 nm light [13]. For irradiated soot and NaCl, agglomerated particles with $D_f \sim 3$ are mainly observed. Their initial particle volume is two orders of magnitude larger than polystyrene and gold, so nucleated nanospheres tend to agglomerate since these processes are concentration dependent. The spherical agglomerates are formed by particle-cluster aggregation in a reaction-limited regime (Eden growth) [14]. Since nucleated particles with the same charge repel each other, only particles with sufficient energy to overcome the electrostatic barrier form spherical agglomerates. These observations suggest that the precursor particles with an initial volume less than $10^{12} \text{ nm}^3/\text{cm}^3$ should be used in the applications where unagglomerated particles are desirable.

The size distributions of the nanoparticles after ablation are highly repeatable. Formation of the new small particles depends on the concentration of gas phase species created by ablation, which is changed by varying the laser conditions. The final particle mean diameter and number concentration are determined by competition between particle production and loss mechanisms. For all the particles studied, the diameter and number concentration increase with PAR without significant particle volume change when irradiated by a single laser pulse. More gas phase species are generated from original particles with increasing PAR, leading to an increase of particle diameter and number concentration. In contrast, particle diameter and number concentration of polystyrene and soot irradiated by multiple laser shots decrease with PAR, with an increasing loss of total volume. The volume lost of polystyrene is likely due to formation of particles $< 13 \text{ nm}$ and stable gas phase species that do not convert to particulate matter, whereas soot is lost because of oxidation. A previous two-laser study showed that soot oxidation after UV ablation is completed within 500 ns, which is faster than the particle nucleation time ($\geq 50 \mu\text{s}$) [1,11]. Although the loss mechanisms are different in polystyrene and soot, significant loss of particle volume when disintegrated by multiple shots results in a decrease of particle diameter and number concentration. A closer examination revealed that for both of these particles, the volume and mean diameter of newly-created small particles start decreasing above a $\text{PAR} = 0.1$, where the loss mechanisms exceed particle nucleation.

In the case of NaCl and gold, the particle diameter and number concentration increase for all the laser conditions examined since there are no significant loss mechanisms. When each NaCl particle was irradiated by 4 or 8 laser shots, no significant differences were observed in the final size distributions [7]; in both cases about twice the volume of small particles was formed as in the single shot case. Since particle nucleation is faster than the time between the pulses ($> 10 \text{ ms}$), the gas phase NaCl after the 1st ablation pulse nucleates and agglomerates before the next pulse arrives. Single shot ablation produces several times smaller particles at a much higher concentration (Fig. 1), and these particles interact with the incident light differently than the original particles; the new small particles can be fully photolyzed while larger particles are partially disintegrated. Note that for the same material, smaller particles have a higher PAR value than larger ones at the same fluence condition, as the PAR is inversely proportional to the particle diameter. Therefore, the particle size distribution after multiple shots is different from that after single pulse ablation even when there is no particle loss. More than 4 shots/particle do not make any significant difference in the final size distribution, since the particles experience repetitive disintegration and condensation. Because of this, we do not report the PAR values of NaCl particles irradiated by multiple shots (Table 1).

One should note that laser ablation of nanoparticles is different from ablation of bulk materials in that not only is the optical breakdown threshold orders of magnitude higher, but the particles produced can be better controlled. The photoproducts from bulk materials include a mixture of gaseous species, hot electrons, and various sized particles in an extreme thermal condition, whereas low temperature gas phase species are produced by UV photolysis of nanoparticles. The concentration of the photolyzed species is the major parameter to control the final particle diameter and morphology, which also makes analysis easier. We use PAR as a metric of the particle volume that is photolyzed, as overall photochemical quantum yield of 193 nm light is very high. Simple gas kinetic theory predicted the irradiated particle diameters and a reasonable agreement was found between the predicted and observed diameters [8,9]. Although detailed photochemical pathways and the dynamics of the

photolyzed species require more rigorous investigation, UV ablation of nanomaterials shows promise in nanostructure synthesis and analysis.

5. Conclusion

The 193 nm laser ablation of various nanoparticles is analyzed. All the nanomaterials studied are photochemically disintegrated into gas phase species, whose concentration is varied by the laser energy and repetition rate. The photolyzed species undergo nucleation and/or agglomeration (depending on the initial particle volume) to form new smaller nanoparticles. We use the photon-atom ratio (PAR) to evaluate the extent of disintegration and the species concentration. The mean diameter and number concentration of the newly-formed nanoparticles are determined by competition between production and loss mechanisms. The mean diameter and number concentration of polystyrene and soot particles irradiated by a single shot increase with PAR, whereas significant loss of particle volume at higher PAR conditions results in the decrease of particle diameter and concentration. In case of NaCl and gold, larger particles at a higher concentration are observed for all the PARs examined.

Acknowledgements

This work was supported by the EHS Superfund Basic Research Program (Grant No. P42-ES047050-01) from the NIEHS and NIH.

References

- [1] Geohegan D B, Puretzky A A, Duscher G and Pennycook S J 1998 *Appl. Phys. Lett.* **72** 2987
- [2] Liu C, Mao X L, Zeng X, Greif R and Russo R E 2004 *Anal. Chem.* **76** 379
- [3] Lencioni D E 1973 *Appl. Phys. Lett.* **23** 12
- [4] Choi J H, Damm C J, O'Donovan N J, Sawyer R F, Koshland C P and Lucas D 2005 *Appl. Spectrosc.* **59** 258
- [5] Choi J H, Koshland C P, Sawyer R F and Lucas D 2005 *Appl. Spectrosc.* **59** 1203
- [6] Stipe C B, Choi J H, Lucas D, Koshland C P and Sawyer R F 2004 *J. Nanopart. Res.* **6** 467
- [7] Choi J H, Stipe C B, Koshland C P, Sawyer R F and Lucas D 2005 *J. Appl. Phys.* **97** 124315
- [8] Choi J H, Lucas D, Koshland C P and Sawyer R F 2005 *J. Phys. Chem. B* **109** 23905
- [9] Choi J H 2005 *PhD Thesis* University of California, Berkeley
- [10] Garrison B J and Srinivasan R 1984 *Appl. Phys. Lett.* **44** 849
- [11] Stipe C B, Lucas D, Koshland C P and Sawyer R F 2005 *Appl. Opt.* **44** 6537
- [12] Bohren C F and Huffman D R 1983 *Absorption and Scattering of Light by Small Particles* (New York: Wiley Interscience)
- [13] Becker M F, Brock J R, Cai H, Henneke D E, Keto J W, Lee J, Nichols W T and Glicksman H D 1998 *Nanostruct. Mater.* **10** 853
- [14] Ivanenko Y V, Lebovka N I and Vygornitskii N V 1999 *Eur. Phys. J. B* **11** 469